Available online at www.sciencedirect.com
SCIENCE DIRECT®
Journal of Sound and Vibration 273 (2004) 387–407
JOURNAL OF SOUND AND VIBRATION
www.elsevier.com/locate/jsvi

Non-linear vibration analysis of smart composite structures with discrete delamination using a refined layerwise theory

A. Chattopadhyay*, H.S. Kim, A. Ghoshal

Department of Mechanical and Aerospace Engineering, Arizona State University, Tempe, AZ 85287-6106, USA

Received 17 October 2002; accepted 26 April 2003

Abstract

A non-linear vibration analysis procedure has been developed to investigate the dynamic response of composite laminates with embedded and/or surface bonded piezoelectric sensors and multiple finite/discrete delaminations. The objective is to accurately predict the sensor output in the time domain. A recently developed refined layerwise composite theory is used to develop the piezoelectric-mechanical model. A two-way coupled electro-mechanical formulation is used to derive the equations of motion. An adaptive non-linear transient implicit algorithm is used to generate the voltage time history, which is useful in characterizing the presence of delamination. The contact problem of delaminated interfacial surfaces is modelled in terms of fictitious linear springs to provide an accurate description of the transient behavior. The accuracy of the model is validated through comparison with experimental results. The validity of low frequency vibration analysis in detection of delamination(s) from in-situ sensor outputs is also established. It is anticipated that the developed framework will be a useful tool in structural health monitoring studies.

1. Introduction

In designing with composites, it is important to take into consideration imperfections, such as delamination, that are often pre-existing or are generated by external impact forces during the service life. Although extensive research has been conducted in investigating delamination in laminated composites, a vast majority of the research work has focused on the initiation and propagation of delamination under static and fatigue loading and the associated reduction in compressive strength of the structure. However, delamination also affects the dynamic characteristics of composite structures. Although these effects are subtler and have been less

*Corresponding author. Tel.: +1-480-965-9342; fax: +1-602-965-1384.
E-mail address: aditi@asu.edu (A. Chattopadhyay).

0022-460X/$ - see front matter
doi:10.1016/S0022-460X(03)00561-3

studied, it is important to include them in developing a model, which can be used in vibration based damage characterization/detection studies. Campanelli and Engblom [1] studied the effect of delamination on the dynamic characteristics of graphite composite plates. Using eight-noded isoparametric quadratic elements, Parhi et al. [2] studied the dynamic analysis of multiple delaminations in composite twisted plates. Saravanos and Hopkins [3] showed the damped dynamic response of composite laminates with delamination cracks. Shen and Grady [4] studied the free vibration of delaminated composite beam using Timoshenko beam theory. Lee [5] analyzed free vibration characteristics of a delaminated composite beam using a layerwise theory. Nath and Shukla [6] modelled the response of composite plates, subjected to step, ramp and sinusoidal loading using Chebyshev series technique. Their formulation was based on the Mindlin first order shear deformation theory and von-Karman non-linearity. Parhi et al. [7] used the first order shear deformation theory to analyze the free vibration and transient response of multiple delaminated doubly curved composite shells subjected to a hygrothermal environment. Newmark's direct integration scheme was used to solve the transient response. The effect of contact between delaminated interfaces during plate vibration has been ignored in many works. However, this contact can alter the response of the structure, particularly at high frequencies for very large structures, as shown by Kwon and Aygunes [8]. The contact between delaminated interfaces makes the response non-linear, which can be solved by using time-integration methods. However, sudden impact of the delaminated interface creates oscillations in analytical response that destabilizes most numerical methods.

In modelling the displacement field in delaminated composites, classical laminate theory (CLT) and first order shear deformation theory (FSDT) has been used in most of the work [1–8]. Although three-dimensional approaches are more accurate than two-dimensional theories, their implementation can be very expensive for practical applications. The layerwise approach is an alternative since it is capable of modelling displacement discontinuities. However, in its original form, the computational effort increases with the number of plies. A refined higher order theory, developed by Chattopadhyay and Gu [9,10], was shown to be both accurate and efficient for modelling delamination in composite plates and shells of moderately thick construction. A higher order zigzag theory was developed by Cho and Kim [11,12] to model laminated composite plates with multiple delaminations. Recently, Kim et al. [13] developed an improved layerwise theory to investigate interlaminar stresses in smart composite structures.

Limited research has been conducted on investigating the effects of delamination on the dynamic response of smart composite structures. A normal mode solution to model continuous piezoelectric sensor outputs for high frequency acoustic emission from propagating cracks in composite plates was presented by Sundaresan et al. [14,15]. The dynamic response of piezoelectric composite laminates, with through-the-width delamination, was addressed by Chattopadhyay et al. [16,17] using a higher order theory. Since transient response plays an important role in damage identification using vibrational procedures, recently, the transient response of composite plates with self-sensing piezoelectric actuators was modelled by Chattopadhyay et al. using a completely coupled electro-mechanical field formulation and higher order displacement theory [18]. The effect of contact between delaminated interfaces was also modelled using a discontinuous time-integration method by Thornburgh and Chattopadhyay [19]. In this work, only through-the-width delamination was considered. The goal of the present paper is to further extend the above work in an effort to develop a generalized framework for modelling

the vibration response of piezoelectric laminated plates addressing some of the important issues. These include: (1) accurate displacement field capable of capturing interlaminar shear stresses, (2) coupled electro-mechanical field formulation to accurately model the energy transfer, (3) presence of multiple discrete delamination and (4) contact between delaminated interfaces.

2. Mathematical formulation

A completely coupled electro mechanical formulation is used to accurately model the energy transfer between the electrical and the mechanical field. For an elastic system with piezoelectric materials, the linear constitutive relations can be expressed as follows.

$$\sigma_{ij} = c_{ijkl}\varepsilon_{kl} - e_{ijk}E_k, \quad D_i = e_{ijk}\varepsilon_{jk} + b_{ij}E_j, \tag{1}$$

where the quantities ε_{ij} and σ_{ij} denote the components of strain and stress tensors, respectively. The quantities E_i and D_i denote components of electric field and electric displacement, respectively. In Eq. (1), three sets of material coefficients are used to address constitutive characteristics of mechanical and electrical fields as well as the coupling between these fields. The quantities c_{ijkl}, e_{ijk} and b_{ij} represent elastic constants, piezoelectric constants and dielectric permittivity, respectively. In the coupled formulation, the above equations are solved simultaneously and not sequentially (as in the conventional one way coupled model). The resulting constitutive equations model both the piezoelectric and the converse piezoelectric effects. The higher order piezoelectric field [13], which can satisfy the equipotential boundary condition, is used to describe the coupled piezoelectric field as

$$\phi^j(x,y,z) = \phi_0^j(x,y) - (z - z_0^j)E_z^j(x,y) + 4\left(\frac{z - z_0^j}{h^j}\right)^2\left[(z - z_0^j)\left(\frac{\bar{\phi}^j}{h^j} + E_z^j(x,y)\right) - \phi_0^j(x,y)\right], \tag{2}$$

where ϕ_0^j is the potential of a point in the mid-plane of the jth piezoelectric layer. The quantity E_z^j denotes the electric field at mid-plane and the term $-(z - z_0^j)E_z^j$ is used to address the linear potential distribution along the thickness. The last term in Eq. (2) represents the higher order modification, addressing the non-uniform potential variation through the thickness while satisfying the equipotential surface boundary conditions prescribed at the electrodes. The quantity $\bar{\phi}^j$ denotes the potential difference between the top and the bottom electrodes covering the jth piezoelectric transducer, and z_0^j and h^j denote the mid-plane position and the thickness of the jth piezoelectric layer, respectively.

2.1. Layerwise displacement with multiple delaminations

Shear deformation plays an important role in the response analysis of composite structures due to material anisotropy and discontinuities at each interface of the laminae. The form of the displacement field of the perfectly bonded layers is determined by the requirements that the transverse shear stresses should vanish on top and bottom surfaces of the laminate, and should be continuous through the thickness. These conditions can be satisfied by a layerwise zigzag displacement field that accounts for the continuous interlaminar shear stresses through the thickness.

Consider an N-layered laminated composite plate with multiple delaminations. The displacement field of the perfectly bonded layers will account for a zigzag-like form of displacements and an interlaminar continuity of transverse stresses. To achieve this, the displacements of a point with the co-ordinates (x, y, z) are described using the superposition of first order shear deformation and layerwise functions, as shown in Eq. (3). The first order shear deformation is used to address the overall response of the entire laminate. The layerwise functions are used to accommodate the complexity of zigzag-like in-plane deformation through the laminate thickness, and to satisfy the interlaminar shear traction continuity requirement. To model the delamination, the assumed displacement field is supplemented with Heaviside unit step functions, which allows discontinuity in the displacement field. The following displacement field is assumed for a laminated plate with multiple delaminations.

$$\begin{aligned} U_i^k(x,y,z,t) &= u_i(x,y,t) + \phi_i(x,y,t)z + \theta_i^k(x,y,t)g(z) + \psi_i^k(x,y,t)h(z) \\ &\quad + \sum_{j=1}^{N-1} \bar{u}_i^j(x,y,t)\mathrm{H}(z-z_j), \\ U_3^k(x,y,z,t) &= w(x,y,t) + \sum_{j=1}^{N-1} \bar{w}^j(x,y,t)\mathrm{H}(z-z_j), \end{aligned} \tag{3}$$

where the superscript k denotes the kth layer of the laminate. The subscript i denotes the co-ordinate x or y. The unknowns are u_i, ϕ_i, w, θ_i^k, ψ_i^k, $\bar{u}_i^j$ and $\bar{w}^j$. Note that u_i and w denote the displacement of the reference plane, ϕ_i are rotations of the normal to the reference plane about the x and y axes. θ_i^k and ψ_i^k are layerwise structural unknowns defined at each laminae. The terms $\bar{u}_i^j$ and $\bar{w}^j$ represent possible jumps in the slipping and opening displacement and z_j denotes the delaminated interface. The function $\mathrm{H}(z-z_j)$ is the Heaviside unit step function. All interfaces between layers are initially assumed to be delaminated. Then, the number of delaminated layer interfaces is equal to the number of the whole interfaces. The perfectly bonded interfaces can be easily simulated by setting $\bar{u}_i^j$ and $\bar{w}^j$ to be zero. The through-laminate-thickness functions, $g(z)$ and $h(z)$ are used to address the characteristics of in-plane zigzag deformation and have the form

$$g(z) = \sinh(z/h), \quad h(z) = \cosh(z/h), \tag{4}$$

where the functions $g(z)$ and $h(z)$ render higher order odd and even distributions, respectively.

There is no need for the use of shear-correction factors in the assumed displacement field. However, the equations provide $5 + 4N + 3(N-1)$ structural unknowns where N is number of layers. The total number of structural unknowns is dependent on the number of layers and delaminations, implying that computational effort will increase greatly if multilayered laminates are used. A reduction in the number of structural variables is essential for the model to be computationally efficient and useful for practical applications. Therefore, a procedure is developed to reduce the number of variables by enforcing continuity of the transverse shear stresses and the in-plane displacement at ply interfaces, as described next.

By imposing surface traction free boundary conditions on top and bottom surfaces of the plate and transverse shear stress and displacement continuity conditions at each interface of laminae, in-plane layerwise displacements of the delaminated composite laminates (Eq. (3)) are

reduced to

$$U_1^k(x,y,z,t) = u_1 + A_1^k(z)\phi_1 + B_1^k(z)\phi_2 + C_1^k(z)w_{,x} + D_1^k(z)w_{,y} + \bar{E}_1^j(z)\bar{w}_{,x}^j + \bar{F}_1^j(z)\bar{w}_{,y}^j + \sum_{j=1}^{N-1}\bar{u}_1^j \mathrm{H}(z-z_j),$$

$$U_2^k(x,y,z,t) = u_2 + A_2^k(z)\phi_1 + B_2^k(z)\phi_2 + C_2^k(z)w_{,x} + D_2^k(z)w_{,y} + \bar{E}_2^j(z)\bar{w}_{,x}^j + \bar{F}_2^j(z)\bar{w}_{,y}^j + \sum_{j=1}^{N-1}\bar{u}_2^j \mathrm{H}(z-z_j), \tag{5}$$

where the layerwise functions $A_i^k(z)$, $B_i^k(z)$, $C_i^k(z)$, $D_i^k(z)$, $\bar{E}_i^j(z)$ and $\bar{F}_i^j(z)$ are obtained from the $4N$ constraint equations and are expressed in term of laminate geometry and material properties ($i = 1, 2$). The detailed procedure can be found in Ref. [20]. The above formulation is implemented using finite element method.

2.2. Finite element implementation

The linear coupled piezoelectric-mechanical problem for a domain V without free body charge, based on displacement and electric potential as independent state variables, can be described using variational principle along with several constraints:

$$\delta\pi(u_i,\phi) = \int_{t_0}^{t} \mathrm{d}t\left\{\int_V (\rho\ddot{u}_i\delta u_i + \sigma_{ij}\delta\varepsilon_{ij} - D_i\delta\phi_{,i})\,\mathrm{d}V - \int_V f_i\delta u_i\,\mathrm{d}V - \int_{\Gamma_\sigma}\bar{t}_i\delta u_i\,\mathrm{d}\Gamma - \int_{\Gamma_D}\bar{q}_e\delta\phi\,\mathrm{d}\Gamma\right\} = 0. \tag{6}$$

Eq. (6) addresses piezoelectric and mechanical fields simultaneously and represents the governing equations of the coupled piezoelectric-mechanical theory. The quantities f_i, $\bar{t}_i$ and $\bar{q}_e$ denote body force, prescribed traction on the stress boundary Γ_σ and surface charge on the charge boundary Γ_D, respectively. In this paper, a four-noded plate element is used with linear Lagrange interpolation functions to describe the in-plane structural unknowns and electrical unknowns and Hermite cubic interpolation functions are used for the out-of-plane unknowns. The above formulation results in 28 generalized nodal unknowns for a undelaminated plate element and $(28 + 5 \times D)$ generalized nodal unknowns for a delaminated element where D represents the number of delamination present. PZT element has 8 nodal unknowns.

After finite element implementation, the governing equations of motion are expressed as

$$\mathbf{M}\ddot{\mathbf{u}} + \mathbf{C}\dot{\mathbf{u}} + (\mathbf{K}_{uu} - \mathbf{K}_{u\phi}\mathbf{K}_{\phi\phi}^{-1}\mathbf{K}_{\phi u})\mathbf{u} = \mathbf{F}_u - \mathbf{K}_{u\phi}\mathbf{K}_{\phi\phi}^{-1}\mathbf{F}_\phi, \tag{7}$$

where u is mechanical displacement unknowns. The matrix $\mathbf{M}$ is the structural mass matrix. The matrices $\mathbf{K}_{u\phi}$ and $\mathbf{K}_{\phi u}$ are stiffness matrices due to piezoelectric-mechanical coupling (converse piezoelectric and piezoelectric effects). Their presence allows piezoelectric materials to produce mechanical actuation forces under input voltages, or electrical signals under mechanical deformations. The matrices $\mathbf{K}_{uu}$ and $\mathbf{K}_{\phi\phi}$, respectively, are stiffness matrices resulting from mechanical and electrical fields. The stiffness coupling effects can influence the equilibrium

position if a steady state exists. The proportional damping is used to define the damping matrix **C**. The vectors $\mathbf{F}_u$ and $\mathbf{F}_\phi$ are force vectors due to mechanical and electrical fields, respectively.

During vibration the delaminated region opens up a little, forming a gap between the laminates and then the laminates come back together, impacting each other at that delaminated interface. This is phenomenon is referred to as 'breathing' of a delamination. In order to capture the true response of a plate during vibration, it is important to model the possibility of contact between the laminates in the delaminated region. The contact between the laminates makes the response a non-linear problem and time integration methods are generally used to study the dynamic response. To represent contact between the laminates, upper and lower laminate interfaces are assumed to be connected by a fictitious spring. This spring is assumed to have zero stiffness under tension and stiffness proportional to the transverse Young's modulus of the plate when subjected to compression. This is a typical method often used by other researchers modelling the buckling of composite laminates with delamination [21,22]. The contact stiffness values are added to the existing system as

$$\mathbf{M}\ddot{\mathbf{u}} + \mathbf{C}\dot{\mathbf{u}} + (\mathbf{K}_{uu} - \mathbf{K}_{u\phi}\mathbf{K}_{\phi\phi}^{-1}\mathbf{K}_{\phi u})\mathbf{u} + \mathbf{K}_{ctc}\mathbf{u} = \mathbf{F}_u - \mathbf{K}_{u\phi}\mathbf{K}_{\phi\phi}^{-1}\mathbf{F}_\phi, \tag{8}$$

where the matrix $\mathbf{K}_{ctc}$ is the contact stiffness matrix. This constant stiffness value is added to opening displacement $\bar{w}^j$. The matrix $\mathbf{K}_{ctc}$ will change over time as the laminates come in contact with each other and then open up. The bimodularity of the contact springs makes the contact problem non-linear and an adaptive modified Newmark-beta implicit non-linear algorithm with Newton–Raphson iteration [23,24] is used to study the response of the composite laminated plate when contact between the laminates is allowed. The numerical algorithm is modified to be a predictor and corrector method during contact between laminates. The non-linear adaptive computational method initially computes the location of the upper and the lower laminate nodal positions. When the delamination is open, the spring stiffness is considered to be zero. However, if the predictor shows contact between the upper and lower delaminated nodal positions, i.e., during closure of the delamination, then contact stiffness is added to the equation of motion. The computational algorithm then computes the corrected nodal positions of the upper and lower laminates interfaces showing the contact between the delaminated interfaces accurately. This adaptive algorithm is easy to implement and avoids the oscillations that had been observed for contact problems when conventional Newmark-beta method had been applied [19].

3. Results and discussion

In the numerical analysis, $[0/90]_{4s}$ carbon cyanate cantilever plates, with discrete delamination (Fig. 1) are considered. The material properties are as follows: $E_1 = 380\,\text{GPa}$, $E_2 = 16.6\,\text{GPa}$,

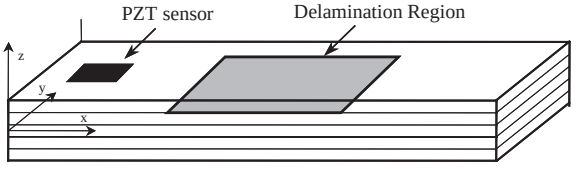

Fig. 1. Geometry of delaminated plate.

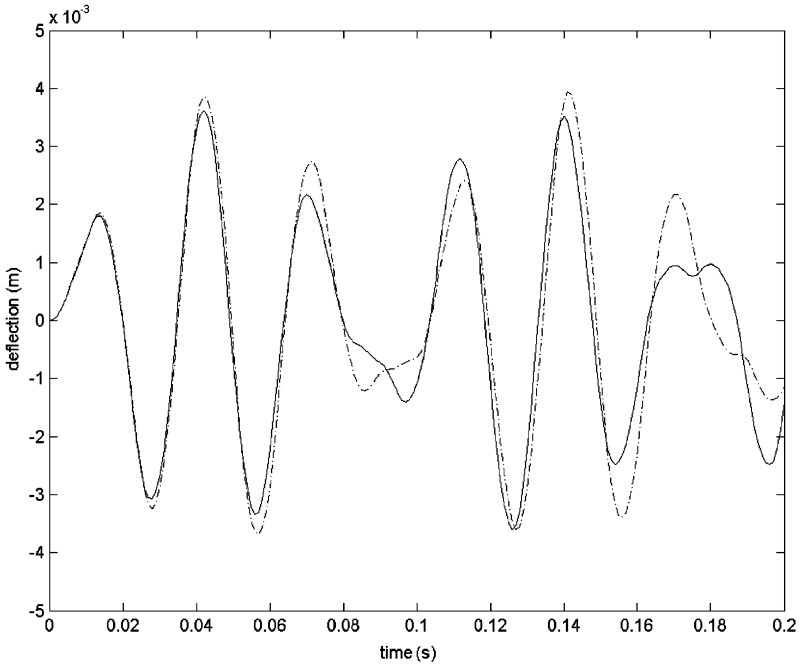

Fig. 2. Time history of tip deflection of the undelaminated and delaminated plate. —, undelaminated plate and –·–, delaminated plate.

$G_{12} = 4.2\,\text{GPa}$, $\rho = 1800\,\text{kg/m}^3$, $v_{12} = 0.31$, $v_{23} = 0.42$. The dimensions of the cantilever plates are length = 30.5 cm, width = 5 cm and thickness = 0.218 cm. A delamination of size 10.4 cm × 5 cm is seeded at a distance of 10.4 cm from the fixed end. The ply level location of delamination is the second interface from the mid surface. A piezoelectric sensor, of size 5 cm × 2.5 cm × 0.025 cm, surface bonded 1 cm away from the fixed end, is used to detect the voltage output when the plate is excited by external loads. The material properties of the lead zirconate titanate (PZT) are as follows: $E = 63\,\text{GPa}$, $\rho = 7700\,\text{kg/m}^3$, and $v = 0.28$. The piezoelectric charge constant (d_{31}, d_{32}) is 250 pm/V and dielectric permittivity is 15.3 nf/m.

First, the plate is excited using a 30 Hz sinusoidal load of 1 N applied at the corner tip of the plate. A finite element mesh consisting of 30×4 four-noded plate elements is used to model the single delamination. Fig. 2 shows the time history of the tip displacement of the plate with and without delamination. The difference in the transient response of the delaminated plate compared to the undelaminated plate is attributed to the shift in natural frequencies due to the presence of delamination. Fig. 3 shows the time-displacement history of upper and lower laminates at the center of the delaminated region under the same load. To observe the 'breathing' phenomena caused by the presence of delamination, the displacements are magnified by a factor of 10^5. Clearly the crests show the 'closure' of the delamination (contact of the interfaces) and the troughs indicate the 'opening' of the delamination. Fig. 4 shows the voltage–time history output of the PZT sensor, which is bonded onto the plate. In this particular case of cantilever plate, under sinusoidal loading tip excitation, sensor output shows exactly same trends as the time history of the tip displacement.

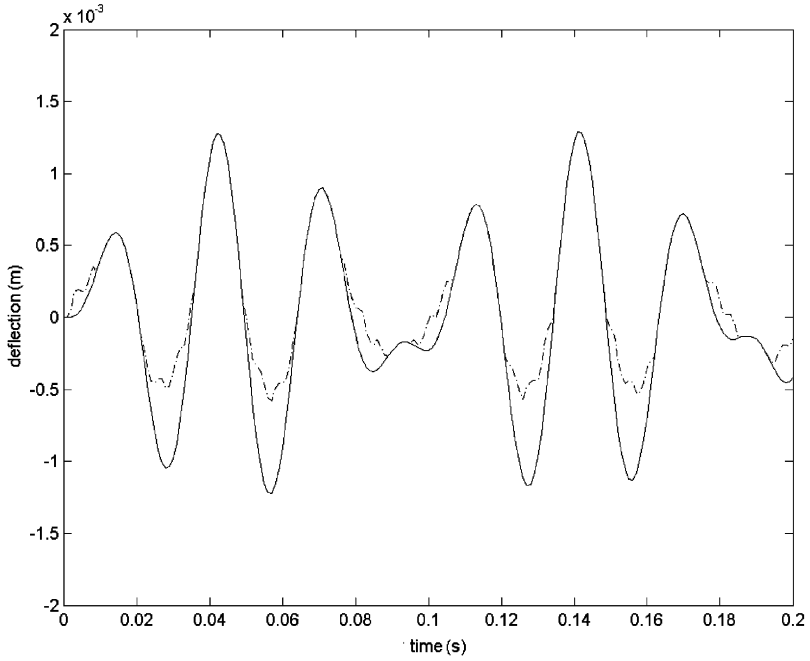

Fig. 3. Time-displacement history of upper and lower delaminated laminates. —, lower laminate and –·–, upper laminate.

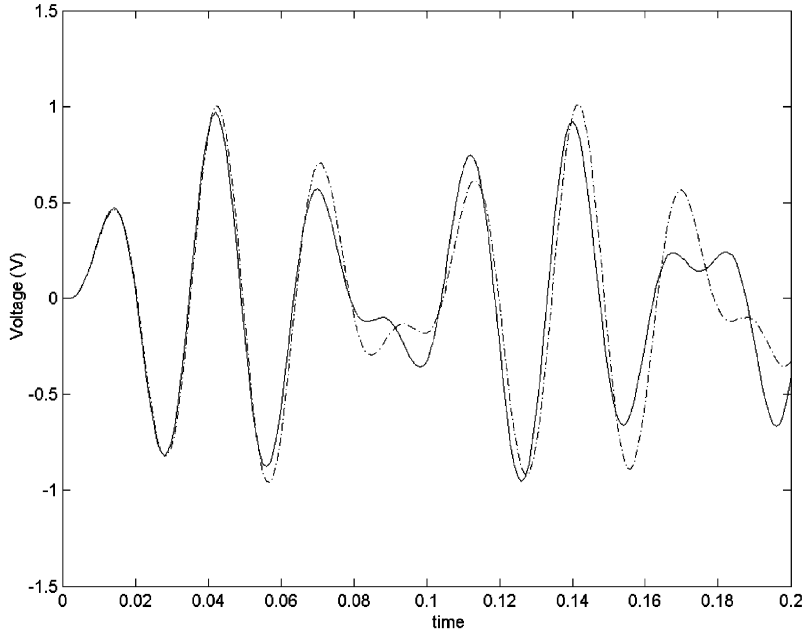

Fig. 4. Sensor output of the undelaminated and delaminated plate. —, undelaminated plate and –·–, delaminated plate.

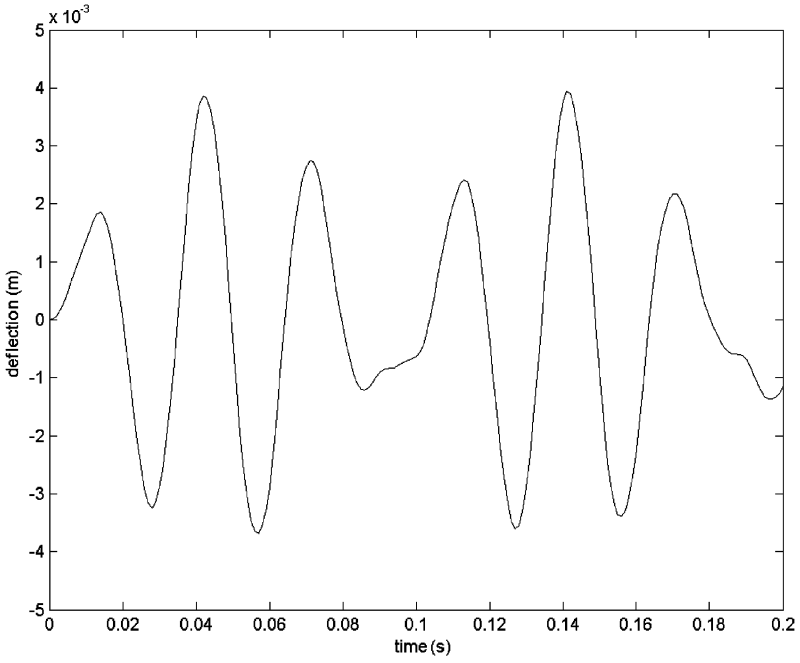

Fig. 5. Time history of tip deflection of delaminated plate without contact excited by sine 30 Hz loading at the tip.

To exemplify the effect of the contact-impact, the above cantilever plate is modelled next without the contact effect included in it. Fig. 5 presents the time history of tip deflection of the delaminated plate excited by a 30 Hz sinusoidal loading of magnitude 1 N, applied at the corner tip. Fig. 6 shows the time history of upper and lower delaminated laminates interfaces without the contact model, magnified by a factor of 10^5. It can be seen that the upper and lower laminates intersect each other during vibration, which is physically meaningless. This shows the importance of including the contact effect in modelling the damage response of delaminated composite laminates. The sensor output of delaminated plate without the contact model is presented in Fig. 7. Although comparison with Fig. 4 shows that there is hardly any difference observed in the voltage output of the sensors, with and without contact model, in order to understand the mechanics of the delamination behavior under vibration, the contact model must be included to accurately represent the mechanics of such vibrating delaminated composite structure.

Next, the transient response of the delaminated plate subjected to impulse load is investigated. An impulse load of magnitude 1 N and duration 5 ms is applied at the corner tip of the free edge of the plate. Time histories of tip displacement of the cantilever plate, with and without delamination, are presented in Fig. 8. The transient response of the plate shows the shift in natural frequencies due to the presence of delamination. This shift in natural frequencies can be observed clearly in the frequency response shown in Fig. 9. The frequency shift associated with the first flexural mode is small. However, it is quite significant in the first twisting mode. Voltage outputs of the PZT sensor, with and without delamination, are presented in Fig. 10. The natural frequency shift is responsible for the out of phase voltage outputs of the sensor bonded onto the

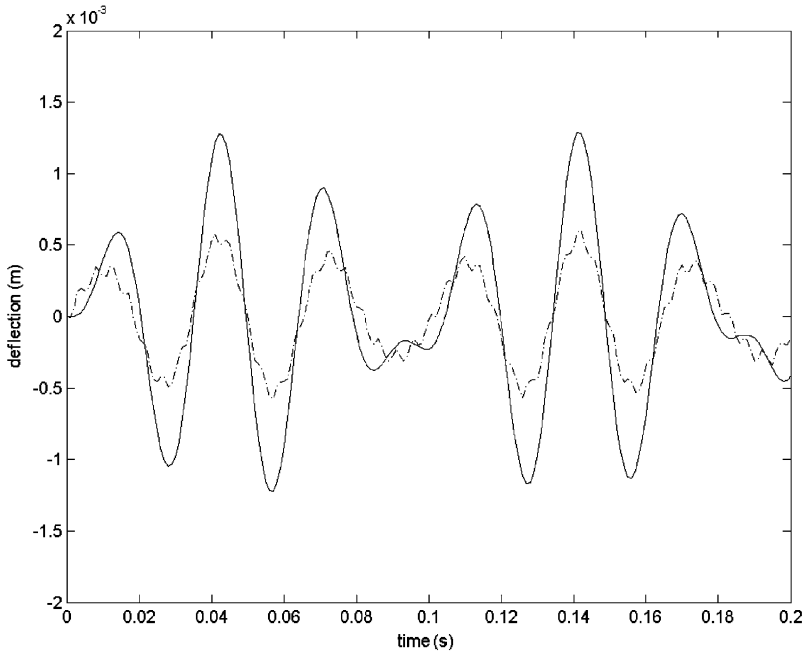

Fig. 6. Time displacement history of upper and lower delaminated laminates interfaces without contact. —, lower laminate and –·–, upper laminate.

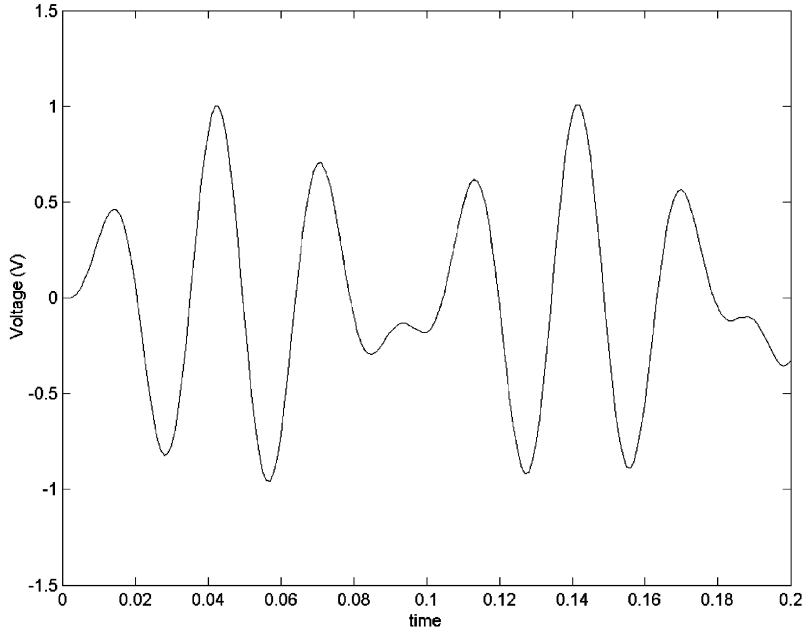

Fig. 7. Sensor output of delaminated plate without contact excited by sin 30 Hz at the tip.

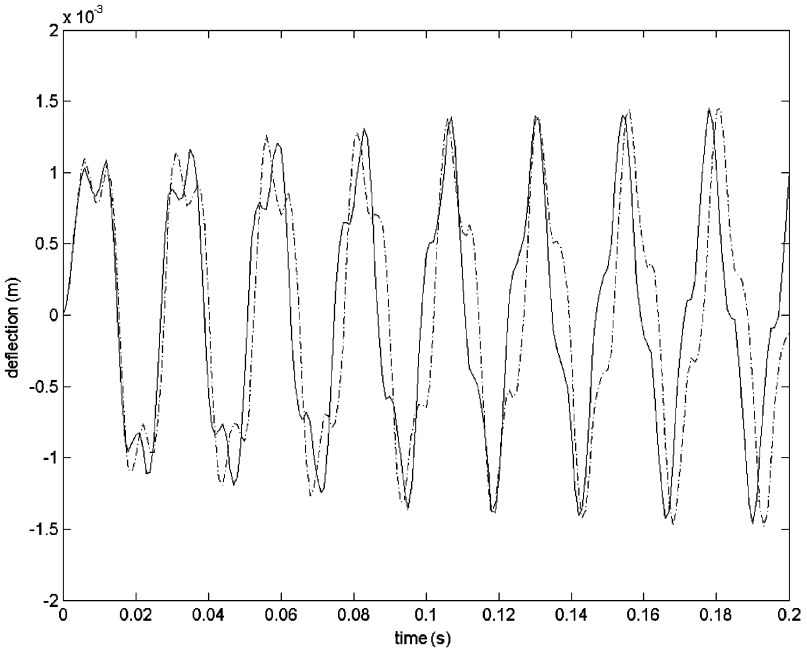

Fig. 8. Time history of tip deflection of undelaminated and delaminated plate. —, undelaminated plate and – · –, delaminated plate.

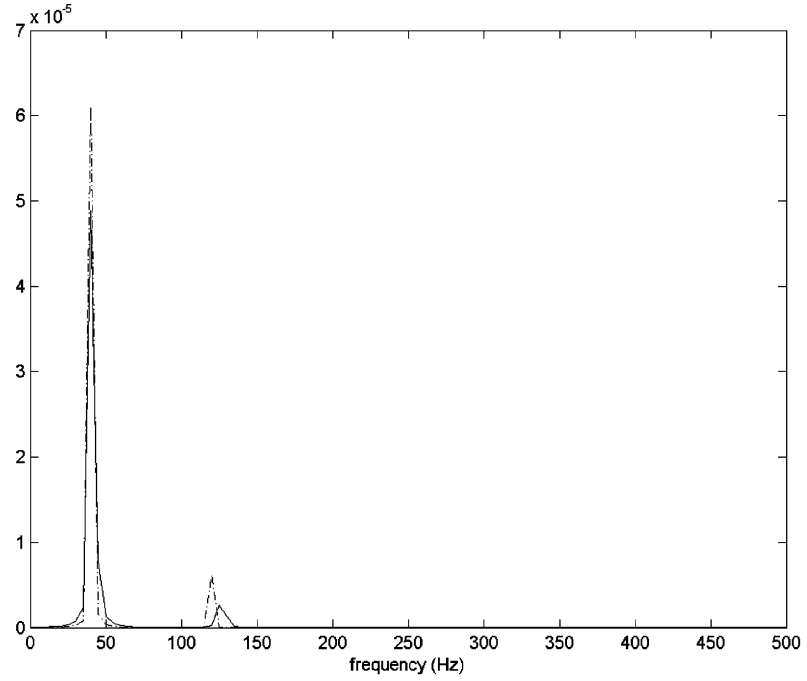

Fig. 9. Frequency response of the undelaminated and delaminated plate. —, undelaminated plate and – · –, delaminated plate.

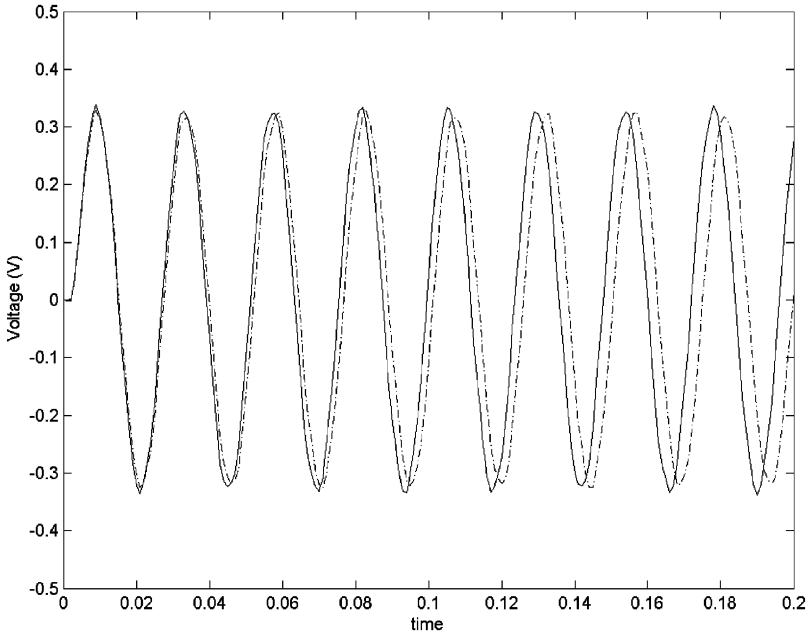

Fig. 10. Sensor output of the undelaminated and delaminated plate. —, undelaminated plate and –·–, delaminated plate.

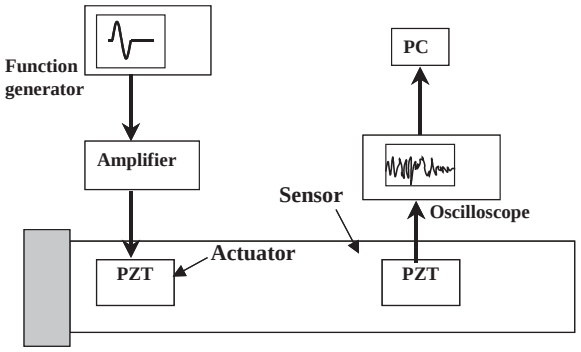

Fig. 11. Experimental setup and plate geometry for transient analysis

delaminated plate with respect to the voltage output from the sensor bonded onto the undelaminated plate (Fig. 11)

Experimental validation of the present analysis is conducted by comparing the voltage–time history output from the PZT sensor. An additional PZT patch is surface bonded at a distance of 19.5 cm away from the fixed end onto the same laminated composite cantilever plate as shown in Fig. 8. This additional sensor is used to detect the voltage output when the plate is excited by external loads. Low frequency excitation voltage is applied on the PZT actuator located near the fixed end. Fig. 12 shows comparison between experimental and numerical voltage output from the undelaminated plate. The PZT actuator is excited by a 20 Hz sinusoidal input with 100 V

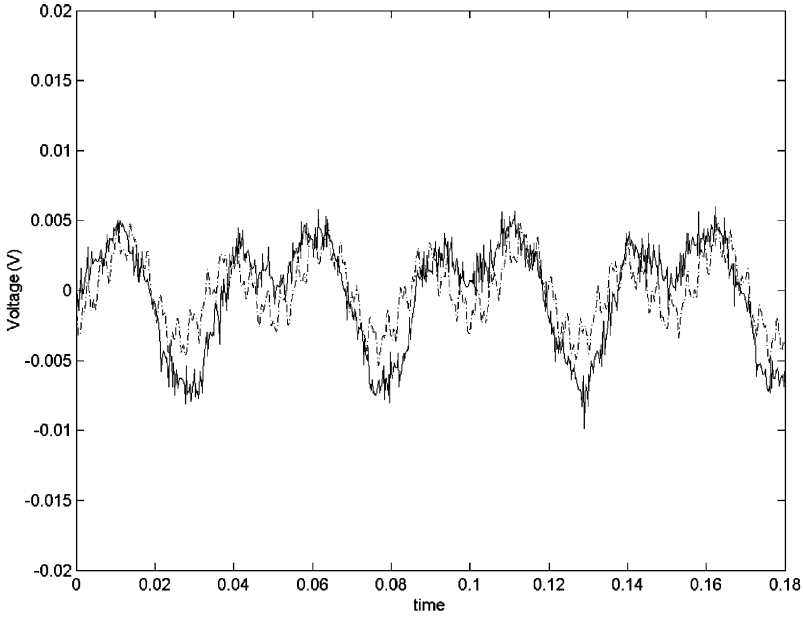

Fig. 12. Voltage output of PZT sensor of undelaminated plate exited by 20 Hz voltage input. —, experiment and –·–, present method.

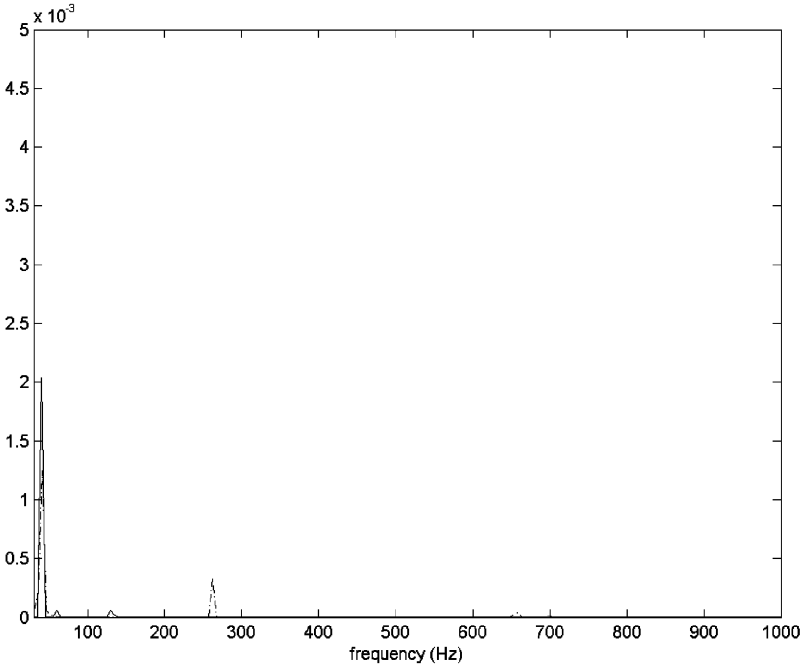

Fig. 13. Frequency response of sensor output of undelaminated plate. —, experiment and –·–, present method.

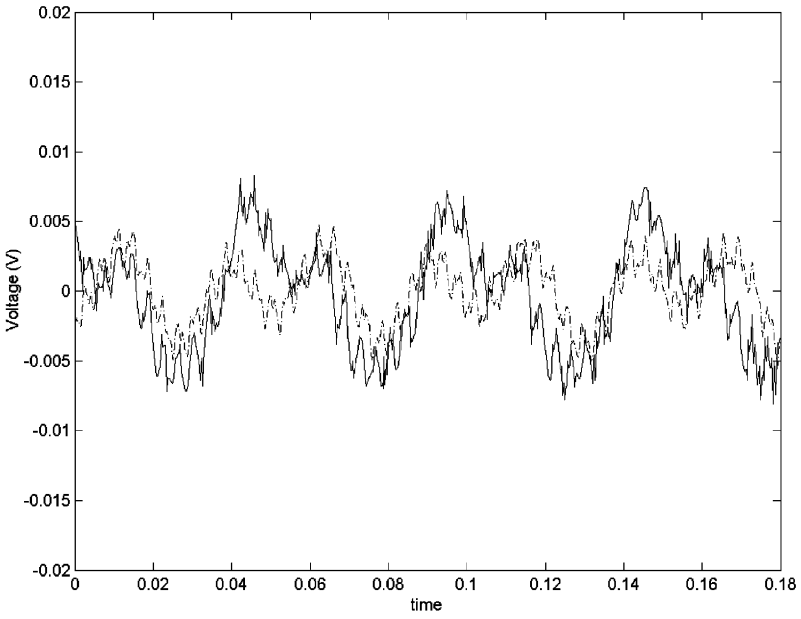

Fig. 14. Voltage output of PZT sensor of delaminated plate exited by 20 Hz voltage input. —, experiment and –·–, present method.

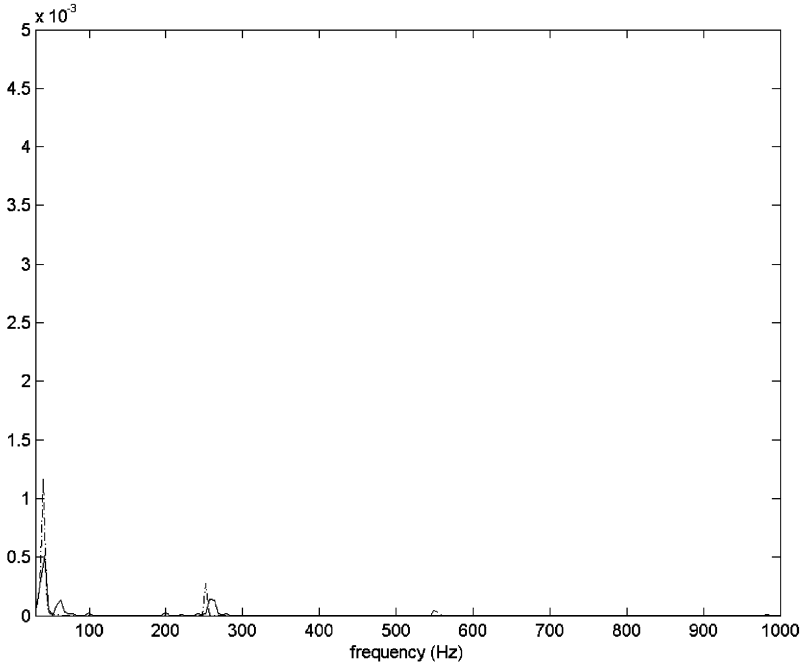

Fig. 15. Frequency response of sensor output of delaminated plate. —, experiment and –·–, present method.

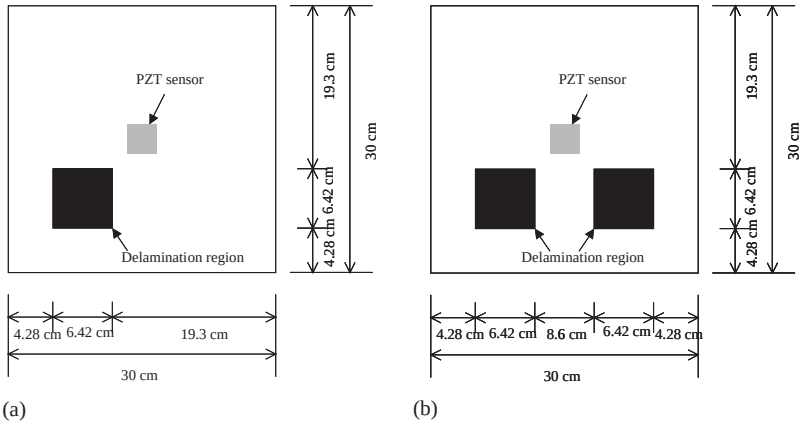

Fig. 16. Geometry of a simply supported square laminated composite plate: (a) with single discrete delamination (D1), (b) multiple discrete delaminations (D2).

amplitude. Fig. 13 shows comparison of the frequency content of the sensor outputs. Similar comparisons for the delaminated plate are presented in Figs. 14 and 15. These figures show good correlation between the experiments and simulation. The slight differences can be attributed to experimental noise (e.g., simulation of the clamped boundary condition, positioning of sensor and actuator) and assumptions made in the analysis (e.g., perfect bonding of sensor/actuator, finite element mesh).

Next, the effects of single and multiple finite delaminations are addressed using a set of carbon cyanate $[0/90]_{4s}$ square plates (30 cm × 30 cm and 0.218 cm thickness) with all edges clamped (Fig. 16). A piezoelectric sensor of size 4.3 cm × 4.3 cm × 0.025 cm, surface bonded at the center of the square plate, is used to detect the voltage output when the plate is excited by external loads. A delamination of size 6.42 cm × 6.42 cm is seeded at a distance of 4.28 cm from the fixed end and located at the second ply interface (from mid surface). A finite element mesh consisting of 14 × 14 four-noded plate elements is used in the numerical modelling. First, the plate is subjected to a 200 Hz sinusoidal load with 1 N magnitude applied at the center. Comparative time histories of the center deflection of the undelaminated plate and plates with single discrete delamination (D1) and multiple discrete delaminations (D2) are presented in Fig. 17. Very small differences are observed in the time histories in this case. Unlike the cantilever plate, the natural frequency shifts, due to the presence of delamination, are small for the lower modes. This is due to the change in boundary conditions that leads to increased stiffness and also the smaller delaminated region considered in this example. Fig. 18 shows similar comparisons of voltage outputs from the PZT sensor.

Figs. 19–21 show snap shots of transverse and in-plane displacements of the square plate without delamination and with single (D1) and multiple discrete delaminations (D2) at a time instant $t = 6$ ms. As seen from these figures, it is very difficult to locate the delaminated region by comparing the transverse deflections. However, delamination is clearly observable through comparison of the in-plane displacements even at such low frequency excitation. The contour plots (Fig. 22(a) and (b)), depicting the difference in normalized transverse deflection shape of the delaminated plate with respect to the undelaminated plate clearly indicate the regions of

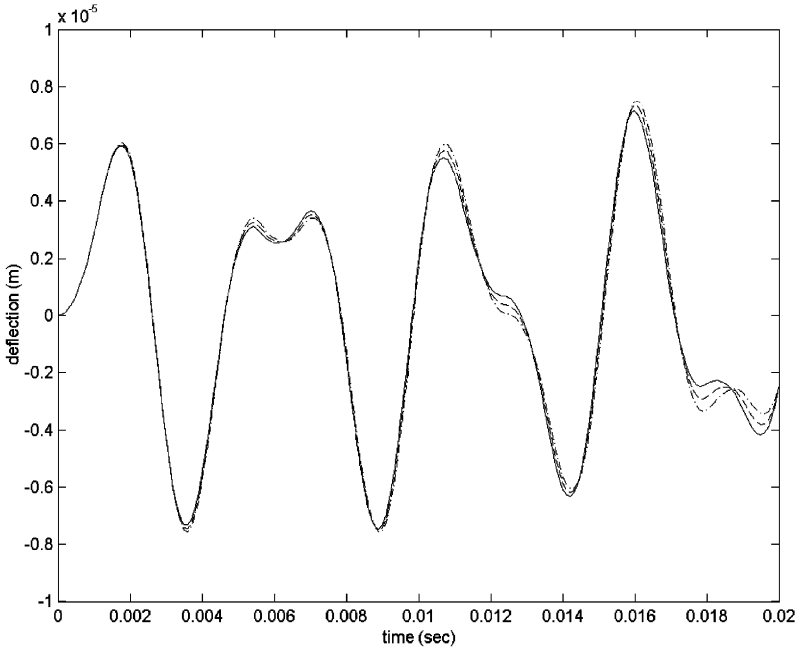

Fig. 17. Time history of center node displacement under 200 Hz sinusoidal loading. —, undelaminated plate; – · –, single discrete delamination (D1) and – –, multiple discrete delaminations (D2).

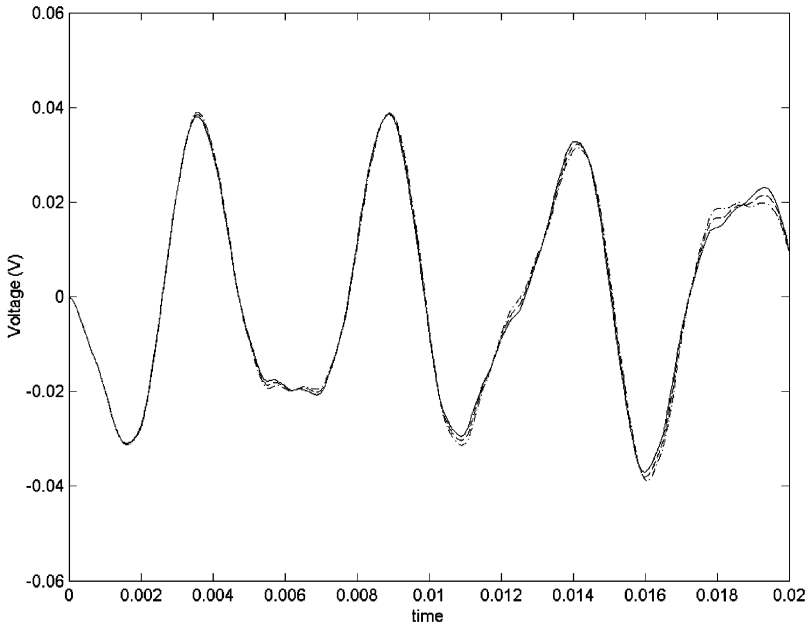

Fig. 18. Sensor output under 200 Hz sinusoidal loading. —, undelaminated plate; – · –, single discrete delamination (D1) and – –, multiple discrete delaminations (D2).

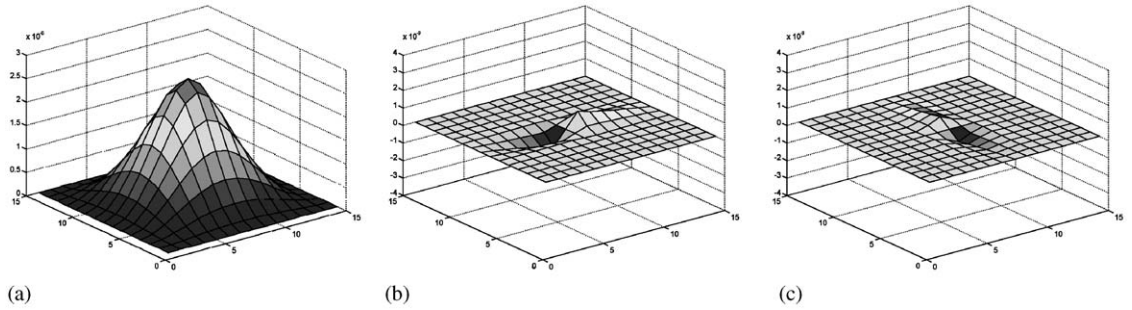

Fig. 19. Structural deformation of undelaminated plate excited by sinusoidal loading of 200 Hz at time instant $t = 6$ ms: (a) transverse deflection (w), (b) in-plane displacement (u), (c) in-plane displacement (v).

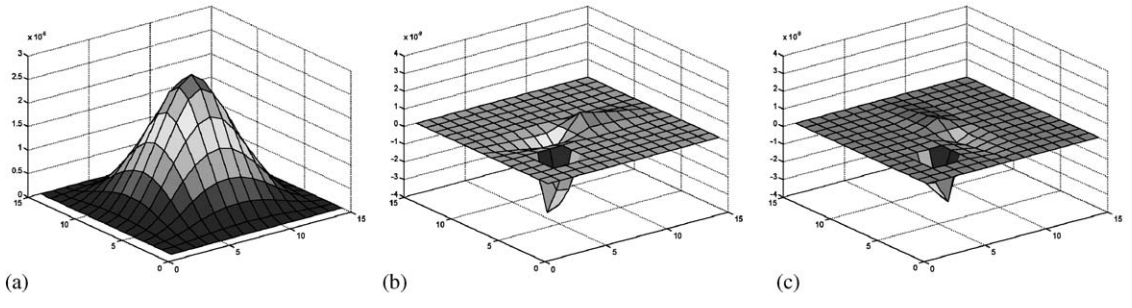

Fig. 20. Structural deformation of single delaminated plate (D1) excited by sinusoidal loading at 6 ms: (a) transverse deflection (w), (b) in-plane displacement (u), (c) in-plane displacement (v).

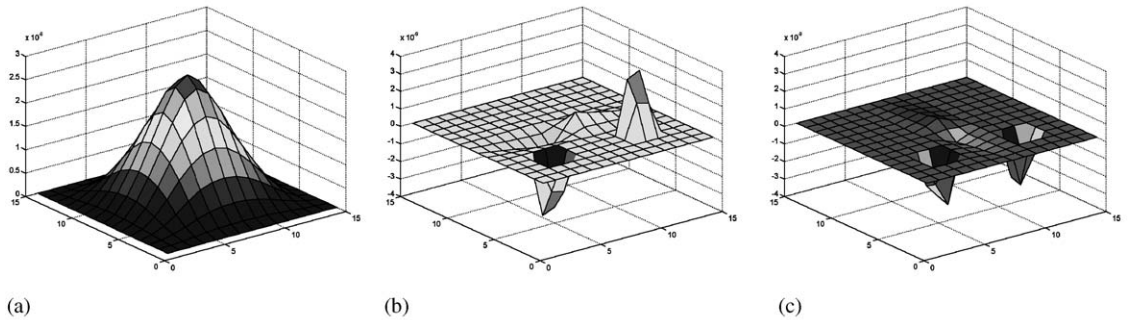

Fig. 21. Structural deformation of multiple delaminated plate (D2) excited by sinusoidal loading at 6 ms: (a) transverse deflection (w), (b) in-plane displacement (u), (c) in-plane displacement (v).

delamination(s). Although the voltage histories from the sensor outputs (Fig. 18) show very small differences, these snapshots seem to indicate that if sensors of appropriate density are surface bonded onto the plate, it is possible to detect the presence of discrete delamination(s) even at such low frequencies.

Next an impulse load of magnitude 1 N and duration 0.5 ms is applied to the center of the square plate. Fig. 23 shows time histories of center deflection of the square plate without

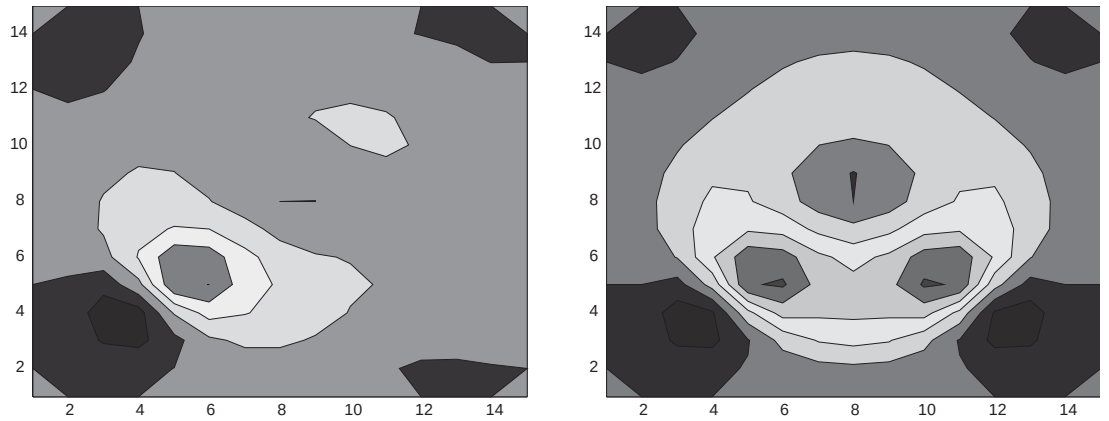

Fig. 22. Contour figures of difference of normalized delaminated vibration deflected shapes with respect to normalized undelaminated vibration deflected shapes: (a) single delamination and (b) two discrete delaminations.

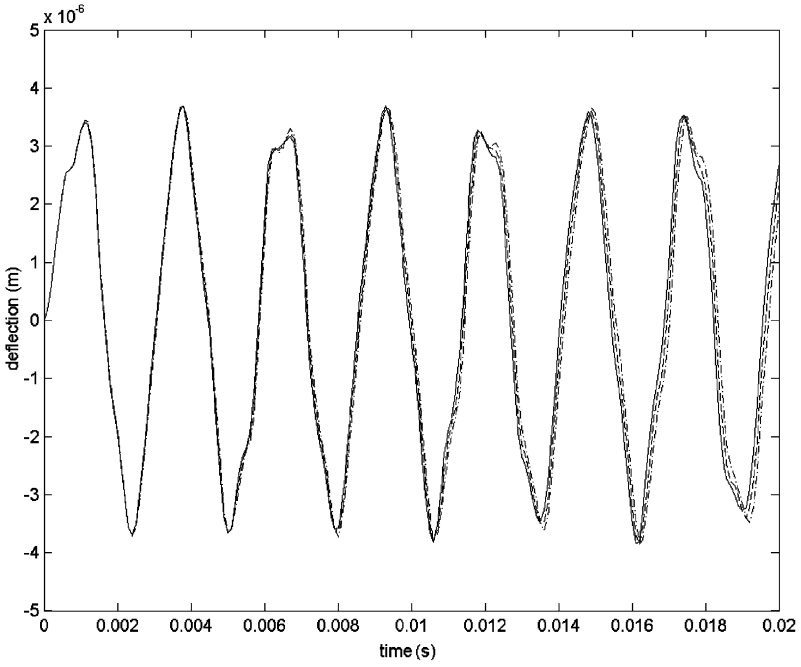

Fig. 23. Time history of center deflection of the square plate under 0.5 ms impulse load. —, undelaminated plate; – · –, single discrete delamination (D1) and – –, multiple discrete delaminations (D2).

delamination and with single discrete delamination (D1) and multiple discrete delaminations (D2). The transient response of the plate also shows the shift in natural frequencies due to the presence of delamination. Frequency responses of the square plate without delamination and with single and multiple discrete delamination(s) are presented in Fig. 24. Voltage outputs of the PZT

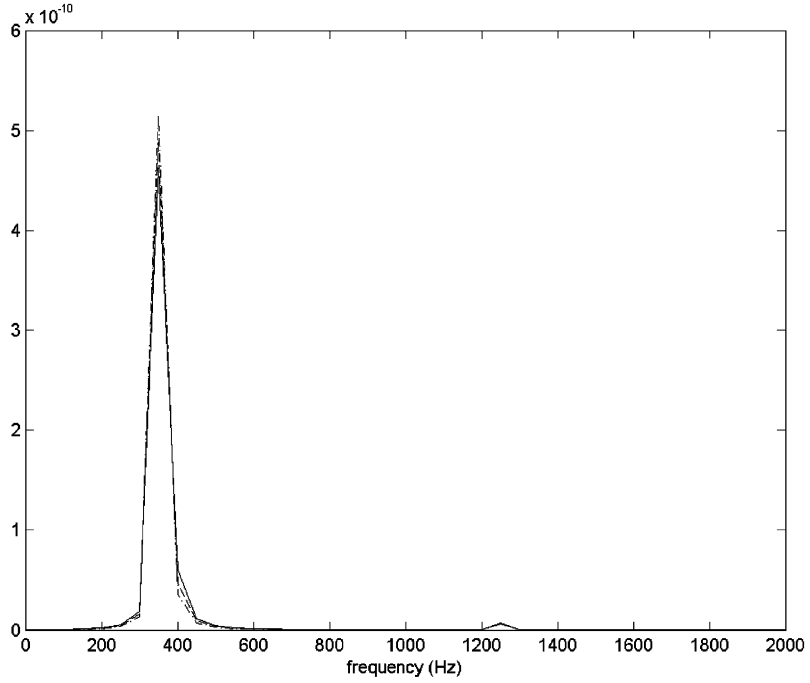

Fig. 24. Frequency response of the square plate under 0.5 ms impulse load. —, undelaminated plate; – · –, single discrete delamination (D1) and – –, multiple discrete delaminations (D2).

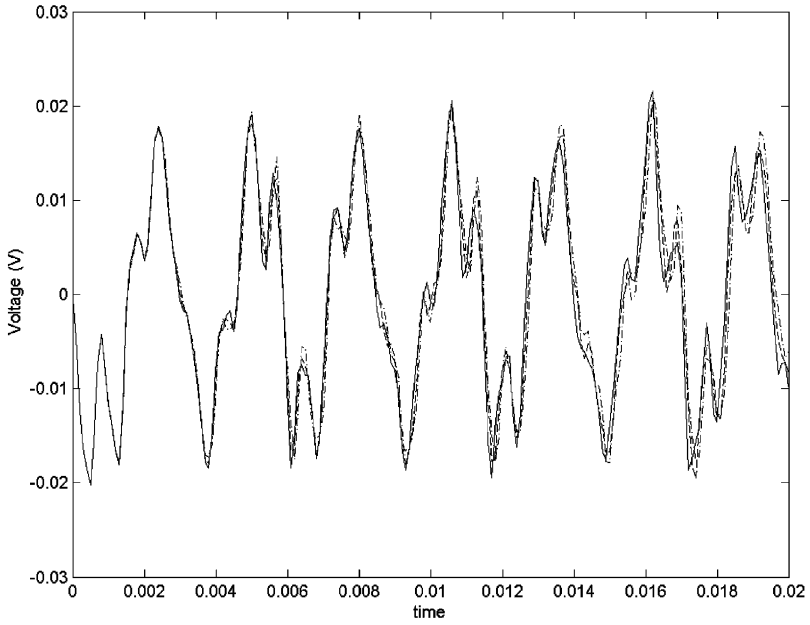

Fig. 25. Sensor output of the square plate under 0.5 ms impulse load. —, undelaminated plate; – · –, single discrete delamination (D1) and – –, multiple discrete delaminations (D2).

sensor during the transient vibration are presented in Fig. 25. It is expected that the out of phase voltage peaks and shifts in the natural frequency would be much more pronounced in higher frequency excitation, or if the delamination regions were larger. It is also expected that detection would be easier if the sensor was placed closer to the delaminated region or if the sensor density on the plate was higher to enable sensors to be placed closer to delaminated zones. Further investigation on sensor location is necessary to obtain better insight about these issues.

4. Concluding remarks

A non-linear vibration analysis procedure has been developed to investigate the dynamic response of composite laminates in the presence of multiple finite delaminations. To characterize the effects of delamination, piezoelectric (PZT) sensors are surface bonded to the host structure to capture the voltage output signal. An improved layerwise laminate theory is used to describe the displacement field, providing accurate stress distributions while maintaining computational efficiency. A completely coupled electro-mechanical formulation is used to derive the equations of motion, which are implemented using finite element method. The contact problem at delaminated interfacial surfaces is modelled in terms of fictitious linear springs to provide an accurate description of the delaminated upper and lower laminates during plate vibration. An adaptive non-linear transient implicit algorithm is used to solve the non-linear response problem. Experiments were conducted to validate the developed model. Following are some important observations that are made from the present study.

1. The numerical and the experimental results show good correlation.
2. The transient response of the plate shows shift in natural frequencies due to the presence of delamination.
3. The contact and non-contact models show little differences in the transient sensor response but it is necessary to model contact for accurate description of upper and lower laminate displacements during vibration.
4. The location of discrete delamination(s) is clearly observable from the distribution of the in-plane displacements.
5. Low frequency analysis can be an effective tool for detection of delaminations using in-situ surface bonded sensor outputs.

Acknowledgements

The research is supported by NASA Langley Research Center, grant number NAG-1-2283, technical monitor Dr. D. Ambur.

References

[1] R.W. Campanelli, J.J. Engblom, The effect of delaminations in graphite/PEEK composite plates on modal dynamic characteristics, *Composite Structures* 31 (1995) 195–202.

[2] P.K. Parhi, S.K. Bhattacharyya, P.K. Sinha, Dynamic analysis of multiple delaminated composite twisted plates, *Aircraft Engineering and Aerospace Technology* 71 (1999) 451–461.
[3] D.A. Saravanos, D.A. Hopkins, Effects of delaminations on the damped dynamic characteristics of composite laminates: analysis and experiments, *Journal of Sound and Vibration* 192 (1996) 977–993.
[4] M.H. Shen, J.E. Grady, Free vibrations of delaminated beams, *American Institute of Aeronautics and Astronautics Journal* 30 (1992) 1361–1370.
[5] J. Lee, Free Vibration analysis of delaminated composite beams, *Computers and Structures* 74 (2000) 121–129.
[6] Y. Nath, K.K. Shukla, Nonlinear transient analysis of moderately thick laminated composite plates, *Journal of Sound and Vibration* 247 (2001) 509–526.
[7] P.K. Parhi, S.S. Bhattacharyya, P.K. Sinha, Hygrothermal effects on the dynamic behavior of multiple delaminated composite plates and shells, *Journal of Sound and Vibration* 248 (2001) 195–214.
[8] Y.W. Kwon, H. Aygunes, Dynamic finite element analysis of laminated beams with delamination cracks using contact-impact conditions, *Computers and Structures* 8 (1996) 1161–1169.
[9] A. Chattopadhyay, H. Gu, A new higher-order plate theory in modeling delamination buckling of composite laminates, *American Institute of Aeronautics and Astronautics Journal* 32 (1994) 1709–1718.
[10] A. Chattopadhyay, H. Gu, Delamination buckling and postbuckling of composite cylindrical shells, *American Institute of Aeronautics and Astronautics Journal* 34 (1996) 1279–1286.
[11] M. Cho, J.S. Kim, Higher-order zig-zag theory for laminated composites with multiple delaminations, *Journal of Applied Mechanics* 68 (2001) 869–877.
[12] J.S. Kim, M. Cho, Buckling analysis for delaminated composites using plate bending elements based on higher-order zig-zag theory, *International Journal for Numerical Methods in Engineering* 55 (2002) 1323–1343.
[13] H.S. Kim, X. Zhou, A. Chattopadhyay, Interlaminar stress analysis of shell structures with piezoelectric patch including thermal loading, *American Institute of Aeronautics and Astronautics Journal* 40 (2002) 2517–2525.
[14] M.J. Sundaresan, A. Ghoshal, M.J. Schulz, An intelligent sensor to measure acoustic waves in plates, *Journal of Intelligent Material Systems and Structures* 12 (2001) 41–57.
[15] M.J. Sundaresan, A. Ghoshal, M.J. Schulz, P.F. Pai, An intelligent sensor for damage detection in bars, *Smart Materials and Structures* 11 (2002) 475–488.
[16] A. Chattopadhyay, H. Gu, D. Dragomir-Daescu, Dynamics of delaminated composite plates with piezoelectric actuators, *American Institute of Aeronautics and Astronautics Journal* 37 (1999) 248–254.
[17] A. Chattopadhyay, D. Dragomir-Daescu, H. Gu, Dynamics of delaminated smart composite cross-ply beams, *Smart Materials and Structures* 8 (1999) 92–99.
[18] A. Chattopadhyay, R. Thornburgh, A. Ghoshal, Transient analysis of smart structures using a coupled piezoelectric-mechanical theory, *IUTAM Symposium on Dynamics of Advanced Materials and Smart Structures*, Yamagata, Japan, 2002.
[19] R. Thornburgh, A. Chattopadhyay, Modeling the dynamic effects of delamination in adaptive composite laminate, *Proceedings of the 43rd AIAA/ASME/ASCE/AHS/ASC Structures, Structural Dynamics and Materials Conference and Exhibition*, Denver, CO, 2002.
[20] H.S. Kim, A. Chattopadhyay, A. Ghoshal, Characterization of delamination effect for laminated composite using a new generalized layerwise approach, *Computers and Structures* 81 (2003) 1555–1566.
[21] G.A. Kardomateas, D.W. Schmueser, Buckling and postbuckling of delaminated composites under compressive loads including transverse shear effects, *American Institute of Aeronautics and Astronautics Journal* 26 (1988) 337–343.
[22] M.J. Pavier, M.P. Clarke, Aspecialized composite plate element for problems of delamination buckling and growth, *Composite Structures* 35 (1996) 45–53.
[23] K.J. Bathe, *Finite Element Procedures*, Englewood Cliffs, Prentice Hall, NJ, 1996.
[24] J. Argyris, H.P. Mlejnek, *Dynamics of Structures*, Elsevier Science, New York, 1991.